Analysis of Microstrip Step Discontinuity by the Modified Residue Calculus Technique

TAK SUM CHU AND TATSUO ITOH, FELLOW, IEEE

Abstract —**The microstrip step discontinuity is analyzed by the modified residue calculus technique. The method is numerically stable and efficient. The results obtained have been compared with other available data, and agreement has been found to be quite good.**

I. INTRODUCTION

ACCURATE INFORMATION on the scattering at the microstrip step discontinuity becomes increasingly important as more precise design procedures are required for monolithic microwave and millimeter-wave integrated circuits. One of the methods for the analysis of the step discontinuity is the mode-matching method applied to the equivalent waveguide model [1]–[4].

In this paper, an alternative technique based on the modified residue calculus technique (MRCT) is presented [5]. It is assumed that the waveguide model is acceptable for the characterization of the step discontinuity. The MRCT is applied to the waveguide model corresponding to the microstrip step discontinuity.

II. FORMULATION

The first step is to find the waveguide model of the step discontinuity. Fig. 1 depicts such a waveguide model. The top and bottom are electric walls and the sidewalls are magnetic walls. The height h is identical to the thickness of the microstrip substrate. The effective dielectric constant ϵ_1 and the effective width $2a$ of Region A can be found from the propagation constant β_1 and the characteristic impedance Z_{01} of the microstripline modeled by the waveguide in Region A.

$$\epsilon_1 = (\beta_1/k_0)^2 \tag{1}$$

$$Z_{01} = \left[120\pi/\sqrt{\epsilon_1}\right](h/2a). \tag{2}$$

β_1 and Z_{01} must be calculated beforehand from the structural parameters by a standard full-wave analysis [6] or a curve fitting formula. Region B can be characterized in the same way.

We now introduce an auxiliary geometry in Fig. 2 that represents one side of the dotted center line in Fig. 1, because we are dealing with a symmetric structure. In this auxiliary geometry, Regions C and D are introduced for convenience of formulation in the MRCT. The original

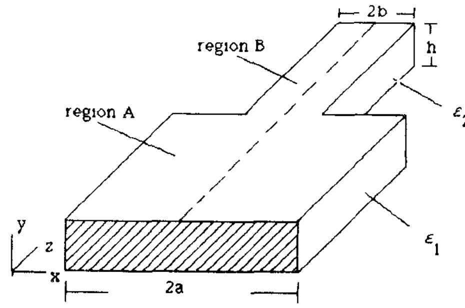

Fig. 1. Equivalent waveguide model of a microstrip step discontinuity.

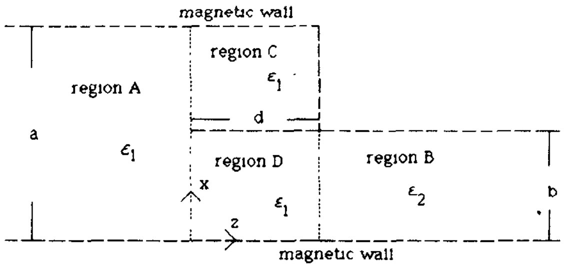

Fig. 2. Auxiliary geometry for analysis.

structure can be recovered by letting $d \to 0$. Notice that the fields are invariant in the y-direction. Then, for the TE_{p0} incidence from Region A and the TE_{q0} incidence from Region B ($p = 0$ or $q = 0$ corresponds to TEM), the E_y field in each regions is

Region A:

$$E_y = A\cos\frac{p\pi x}{a}e^{-j\beta_p z} + \sum_{n=0}^{\infty} A_n \cos\frac{n\pi x}{a}e^{j\beta_n z}, \qquad z < 0$$

Region B:

$$E_y = B\cos\frac{q\pi x}{b}e^{j\gamma_q z} + \sum_{n=0}^{\infty} B_n \cos\frac{n\pi x}{b}e^{-j\gamma_n z}, \qquad z > d$$

Region C:

$$E_y = \sum_{n=0}^{\infty} C_n \cos\frac{n\pi(x-b)}{c}\left[e^{-j\bar{\beta}_n z} + \rho_n e^{j\bar{\beta}_n z}\right], \qquad 0 < z < d$$

Region D:

$$E_y = \sum_{n=0}^{\infty} \cos\frac{n\pi x}{b}\left[D_n e^{-j\bar{\gamma}_n z} + F_n e^{j\bar{\gamma}_n z}\right], \qquad 0 < z < d$$

where A and B are the amplitudes of the incident modes, and A_n, B_n, C_n, D_n, and F_n are the unknown scattered mode amplitudes. Also β_n, γ_n, $\bar{\beta}_n$, and $\bar{\gamma}_n$ are the propa-

Manuscript received February 11, 1985; revised May 14, 1985. This work was supported by U.S. Army Research Office Contract DAAG29-84-K-0076.

The authors are with the Department of Electrical and Computer Engineering, University of Texas, Austin, TX 78712.

0018-9480/85/1000-1024$01.00 ©1985 IEEE

gation constants in the respective region

$$\beta_n = \sqrt{\epsilon_1 k_0^2 - \left(\frac{n\pi}{a}\right)^2} \quad \gamma_n = \sqrt{\epsilon_2 k_0^2 - \left(\frac{n\pi}{b}\right)^2}$$

$$\bar{\beta}_n = \sqrt{\epsilon_1 k_0^2 - \left(\frac{n\pi}{c}\right)^2} \quad \bar{\gamma}_n = \sqrt{\epsilon_1 k_0^2 - \left(\frac{n\pi}{b}\right)^2}$$

$$c = a - b$$

and

$$\rho_n = \exp(-2j\bar{\beta}_n d).$$

Naturally, the corresponding H_x fields can be found from the derivative of E_y with respect to z.

We impose the continuity conditions at $z = d$ and $z = 0$ for the respective E_y and H_x components. Imposing the orthogonality conditions and rearranging the resultant expressions, we obtain a linear simultaneous equation for A_n, B_n, and C_n. When B_n and C_n are eliminated by some algebraic manipulation, the following expressions involving the unknown modal coefficients are obtained:

where

$$\bar{A}_n = \frac{p\pi}{a}\sin\left(\frac{p\pi b}{a}\right)A_n$$

$$\Gamma_m = \frac{\bar{\gamma}_m - \gamma_m}{\bar{\gamma}_m + \gamma_m}, \qquad m = 1,2,3,\cdots$$

$$\Gamma_0 = \frac{\bar{\gamma}_0 - \gamma_0}{\bar{\gamma}_0 + \gamma_0}.$$

Because of the linearity of the set of equations, excitations from Regions A and B can be considered separately. As a demonstration, we will develop the solution for TE_{00} (TEM) excitation from Region A. The solution for the excitation from Region B or for another modal excitation is similar.

For the case in consideration, p, B, and d, are set to zero in the above expressions to obtain the final form of equations for which the MRCT can be applied. The solution for this set of equations is based upon the construction of a meromorphic function $f(w)$ satisfying the following

$$\left[(\beta_p - \bar{\gamma}_0) + \Gamma_0(\beta_p + \bar{\gamma}_0)\right] bA\delta_p^0 - (1-\delta_p^0)\cdot\left[\frac{\frac{p\pi}{a}\sin\left(\frac{p\pi b}{a}\right)}{\beta_p + \bar{\gamma}_0} + \Gamma_0\frac{\frac{p\pi}{a}\sin\left(\frac{p\pi b}{a}\right)}{\beta_p - \bar{\gamma}_0}\right]A$$

$$-\left[(\beta_0 + \bar{\gamma}_0) + \Gamma_0(\beta_0 - \bar{\gamma}_0)\right] bA_0 + \sum_{n=1}^{\infty}\left(\frac{\bar{A}_n}{\beta_n - \bar{\gamma}_0} + \Gamma_0\frac{\bar{A}_n}{\beta_n + \bar{\gamma}_0}\right) = -\left[(\bar{\gamma}_0 + \gamma_0) - \Gamma_0(\bar{\gamma}_0 - \gamma_0)\right] b\delta_0^q B \quad (3)$$

$$-\left[\frac{\frac{p\pi}{a}\sin\left(\frac{p\pi b}{a}\right)}{\beta_p + \bar{\gamma}_m}A + \Gamma_m\frac{\frac{p\pi}{a}\sin\left(\frac{p\pi b}{a}\right)}{\beta_p - \bar{\gamma}_m}A\right] + \sum_{n=1}^{\infty}\left(\frac{\bar{A}_n}{\beta_n - \bar{\gamma}_m} + \Gamma_m\frac{\bar{A}_n}{\beta_n + \bar{\gamma}_m}\right)$$

$$= (-1)^m\frac{b}{2}\left[(\bar{\gamma}_m - \gamma_m)\Gamma_m - (\bar{\gamma}_m + \gamma_m)\right]\delta_m^q B, \quad m = 1,2,3,\cdots \quad (4)$$

$$-\left[(\beta_p - \bar{\beta}_0) + \rho_0(\beta_p + \bar{\beta}_0)\right] c\delta_p^0 A - (1-\delta_p^0)\cdot\left[\frac{\frac{p\pi}{a}\sin\left(\frac{p\pi b}{a}\right)}{\beta_p + \bar{\beta}_0}A + \rho_0\frac{\frac{p\pi}{a}\sin\left(\frac{p\pi b}{a}\right)}{\beta_p - \bar{\beta}_0}A\right]$$

$$+\left[(\beta_0 + \bar{\beta}_0) + \rho_0(\beta_0 - \bar{\beta}_0)\right] cA_0 + \sum_{n=1}^{\infty}\left[\frac{\bar{A}_n}{\beta_n - \bar{\beta}_0} + \rho_m\frac{\bar{A}_n}{\beta_n - \bar{\beta}_0}\right] = 0 \quad (5)$$

$$-\left[\frac{\frac{p\pi}{a}\sin\left(\frac{p\pi b}{a}\right)}{\beta_p + \bar{\beta}_m}A + \rho_m\frac{\frac{p\pi}{a}\sin\left(\frac{p\pi b}{a}\right)}{\beta_p - \bar{\beta}_m}A\right] + \sum_{n=1}^{\infty}\left[\frac{\bar{A}_n}{\beta_n - \bar{\beta}_m} + \rho_m\frac{\bar{A}_n}{\beta_n + \bar{\beta}_m}\right] = 0, \qquad m = 1,2,3,\cdots. \quad (6)$$

B_n can be related to A_n as

$$(\beta_p + \bar{\gamma}_0) b\delta_p^0 A - (1-\delta_p^0)\frac{\frac{p\pi}{a}\sin\left(\frac{p\pi b}{a}\right)}{\beta_p - \gamma_0}A - (\beta_0 - \bar{\gamma}_0) bA_0 + \sum_{n=1}^{\infty}\frac{\bar{A}_n}{\beta_n + \bar{\gamma}_0} = (\bar{\gamma}_0 - \gamma_0) b\delta_0^q B + (\bar{\gamma}_0 + \gamma_0) bB_0 \quad (7)$$

$$\frac{-\frac{p\pi}{a}\sin\left(\frac{p\pi b}{a}\right)}{\beta_p - \bar{\gamma}_m}A + \sum_{n=1}^{\infty}\frac{\bar{A}_n}{\beta_n + \bar{\gamma}_m} = (-1)^m\frac{b}{2}(\bar{\gamma}_m - \gamma_m)\delta_m^q B + (-1)^m\frac{b}{2}(\bar{\gamma}_m + \gamma_m)B_m, \qquad m = 1,2,3,\cdots \quad (8)$$

conditions:

i) $f(w)$ has simple poles at $w=\beta_n, \quad n=1,2,3,\cdots$
ii) $f(\bar{\beta}_m)+f(-\bar{\beta}_m)=0, \quad m=1,2,3,\cdots$
iii) $f(\bar{\gamma}_m)+\Gamma_m f(-\bar{\gamma}_m)=0, \quad m=1,2,3,\cdots$
iv) $f(w)\sim Kw^{-5/3}, \quad$ as $w+\infty$.

Next, let us consider the following contour integrals where c is a circle with an infinite radius:

$$\frac{1}{2\pi j}\oint_C\left(\frac{f(w)}{w-\bar{\gamma}_0}+\Gamma_0\frac{f(w)}{w+\bar{\gamma}_0}\right)dw$$

$$=\sum_{n=1}^{\infty}Rf(\beta_n)\left(\frac{1}{\beta_n-\bar{\gamma}_0}+\frac{\Gamma_0}{\beta_n+\bar{\gamma}_0}\right)$$

$$+f(\bar{\gamma}_0)+\Gamma_0 f(-\bar{\gamma}_0)$$

$$\times\frac{1}{2\pi j}\oint_C\left(\frac{f(w)}{w-\bar{\gamma}_m}+\Gamma_m\frac{f(w)}{w+\bar{\gamma}_m}\right)dw$$

$$=\sum_{n=1}^{\infty}Rf(\beta_n)\left(\frac{1}{\beta_n-\bar{\gamma}_m}+\frac{\Gamma_m}{\beta_n+\bar{\gamma}_m}\right)$$

$$+f(\bar{\gamma}_m)+\Gamma_m f(-\bar{\gamma}_m), \qquad m=1,2,3,\cdots$$

$$\times\frac{1}{2\pi j}\oint_C\left(\frac{f(w)}{w-\beta_0}+-\frac{f(w)}{w+\beta_0}\right)dw$$

$$=\sum_{n=1}^{\infty}Rf(\beta_n)\left(\frac{1}{\beta_n-\beta_0}+\frac{1}{\beta_n+\beta_0}\right)$$

$$+f(\bar{\beta}_0)+f(-\bar{\beta}_0)$$

$$\times\frac{1}{2\pi j}\oint_C\left(\frac{f(w)}{w-\beta_m}+\frac{f(w)}{w+\beta_0}\right)dw$$

$$=\sum_{n=1}^{\infty}Rf(\beta_n)\left(\frac{1}{\beta_n-\beta_m}+\frac{1}{\beta_n+\beta_m}\right)$$

$$+f(\bar{\beta}_m)+f(-\bar{\beta}_m), \qquad m=1,2,3,\cdots$$

where $Rf(w)$ is the residue of f at w.

All of the above contour integrations yield zero because of the asymptotic behavior of $f(w)$ as $|w|\to\infty$. Using conditions i) and ii) and comparing (3)–(6) with (9)–(12), we obtain the following relationships between $f(w)$ and A_n:

$$af\left(\sqrt{\epsilon_1}k_0\right)+(c\Gamma_0+b)f\left(-\sqrt{\epsilon_1}k_0\right)=2\sqrt{\epsilon_1}k_0bc(\Gamma_0-1)A \tag{13}$$

$$A_0=\frac{(\Gamma_0 b+c)f\left(\sqrt{\epsilon_1}k_0\right)+\Gamma_0 af\left(-\sqrt{\epsilon_1}k_0\right)}{2\sqrt{\epsilon_1}k_0bc(\Gamma_0-1)} \tag{14}$$

$$\bar{A}_n=Rf(\beta_n), \qquad n=1,2,3,\cdots. \tag{15}$$

To solve for B_m, we consider the following integrals:

$$\frac{1}{2\pi j}\oint_C\frac{f(w)}{w+\bar{\gamma}_0}dw=\sum_{n=1}^{\infty}\frac{Rf(\beta_n)}{\beta_n+\bar{\gamma}_0}+f(-\bar{\gamma}_0) \tag{16}$$

$$\frac{1}{2\pi j}\oint_C\frac{f(w)}{w+\bar{\gamma}_m}dw=\sum_{n=1}^{\infty}\frac{Rf(\beta_n)}{\beta_n+\bar{\gamma}_0}+f(-\bar{\gamma}_m), \qquad m=1,2,3,\cdots. \tag{17}$$

The left-hand sides would again yield zero. Comparing (7) and (8) with (16) and (17), we arrive at

$$B_0=((\beta_0+\bar{\gamma}_0)bA-f(-\gamma_0))/b(\gamma_0+\bar{\gamma}_0) \tag{18}$$

$$B_m=(-1)^{m+1}2f(-\gamma_m)/b(\gamma_m+\bar{\gamma}_m), \qquad m=1,2,3,\cdots. \tag{19}$$

Hence, once $f(w)$ is constructed, A_m and B_m can be obtained. Let us consider the following functional form of $f(w)$:

$$f(w)=KP(w)\exp(Lw)\frac{\Pi^{Ma}(w,\bar{\beta}_n+\delta)\Pi^{Mb}(w,\bar{\gamma}_n)}{\Pi(w,\beta_n)}$$

where

K = unknown coefficient
L = $j\frac{a}{\pi}\left(\ln\left(\frac{a}{c}\right)+\frac{b}{a}\ln\left(\frac{c}{b}\right)\right)$
δ = $-j(\pi/6c)$
$\Pi(w,\beta_n)$ = $\prod_{n=1}^{\infty}((1-w/\beta_n)\exp(jwb/n\pi))$
Π^M denotes omission of first M factors

and

$$P(w)=\prod_{i=1}^{\infty}(1-w/W_i)+\sum_{i=1}^{M}\left(F_i\prod_{\substack{j=1\\ j\neq i}}^{M}\left(\frac{w-W_j}{W_i-W_j}\right)\right)$$

where

$$M=M_a+M_b$$
$$W_i=\bar{\beta}_i, \qquad i=1,2,3,\cdots,M_a$$
$$W_{i+M_a}=\bar{\gamma}_i, \qquad i=1,2,3,\cdots,M_b.$$

Since K can be determined from the normalization condition (13), the only unknowns are coefficients F_i, which can be determined by imposing conditions ii) and iii). From this process, linear simultaneous equations for F_i with the coefficient matrix size $M\times M$ are derived. They are solved for F_i.

It should be noticed that, as is well known, the canonical bifurcation problem obtained by $d\to 0$ in Fig. 2 cannot be solved by the residue calculus technique if the excitation from A is TEM because the TEM mode does not excite the higher order mode.

III. Numerical Results

Convergence of the present numerical method has first been studied by increasing the matrix size M. Fig. 3 plots the magnitude of the transmission coefficient of the dominant mode into Region B with the dominant mode incident

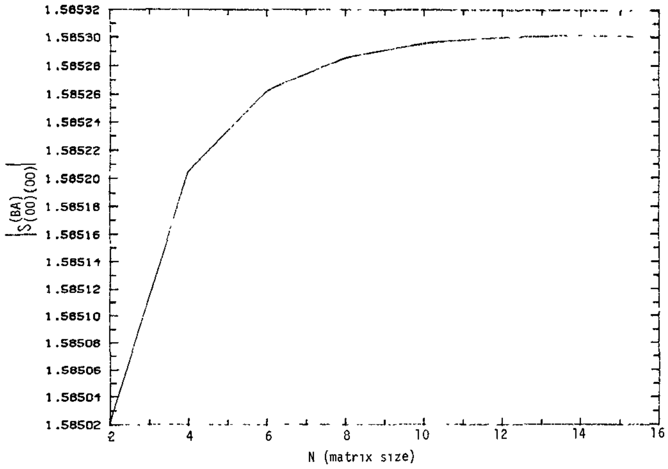

Fig. 3. Convergence study of the method.

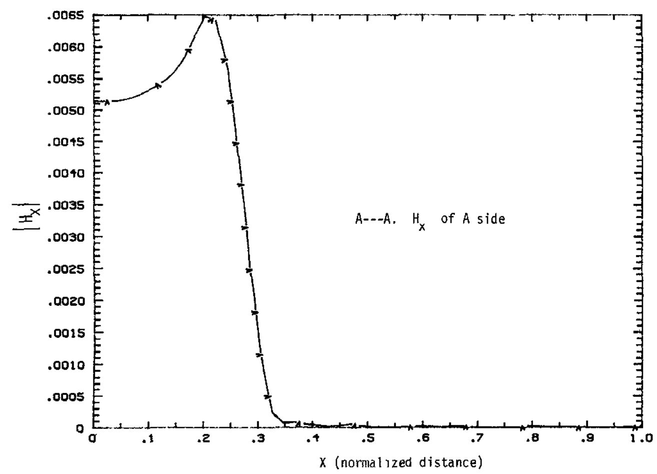

Fig. 4. Magnetic field distribution at the discontinuity. Dominant mode incident from Region A. Matrix size $M = 12$.

from Region A. In this case, $M_a = M_b$ has been maintained. The structural parameters are $a = 100$, $b = 26.1$ (in mils), $\epsilon_1 = 2.2$, and $\epsilon_2 = 2.1$. Notice that the vertical scale is extremely expanded so that the change in the fifth decimal place can be observed. The number of terms in the truncated infinite products is 40 in this case.

Fig. 4 shows the magnitude of the H_x field at $z = 0$. The curve indicates the singularity nature of the H_x near the edge and the satisfaction of the boundary condition $H_x = 0$ on the magnetic wall $b(26.1) < x < a(=100)$.

In addition, the numerical efficiency and stability of the present method are compared to those of the mode matching method [4]. Table I shows the convergence trend of the dominant mode reflection coefficient. Since the two methods are essentially different, the computation time should be compared in addition to the matrix size. The computation was run on a CDC 170/750 at the Computation Center of the University of Texas. The matrix size used was 8×8 for both methods. The average computation time for each frequency point for the mode-matching method is 0.30 s, and it is 0.27 s for the MRCT.

In Fig. 5, the frequency characteristics of the reflection and transmission coefficients calculated by the present method are compared with those reported by Kompa [2]. A slight discrepancy is caused by the use of different dispersion formulas to calculate the effective dielectric constants and the effective widths.

TABLE I
COMPARISON OF CONVERGENCE

Matrix size	$\lvert S^{AA}_{[00][00]}\rvert$ MRCT	Mode-Matching
2	59935	59947
4	59930	59934
6	59930	59930
8	59929	59929
10	59929	59928
12	59929	59928
14	59929	59928

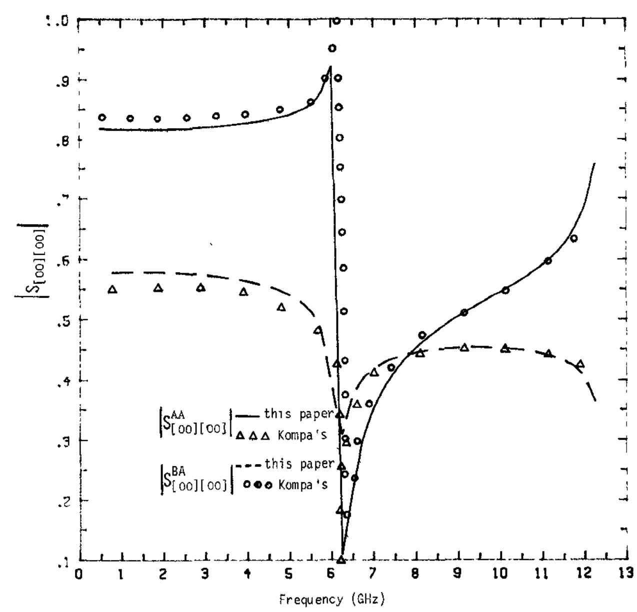

Fig. 5. Frequency-dependent characteristics of the scattering parameters.

IV. Conclusion

The modified residue calculus technique has been applied to the symmetric microstrip step problem. The results can be computed efficiently and accurately. This method is useful for the step discontinuity structure for which the equivalent waveguide model is a valid approximation.

References

[1] I. Wolff, G. Kompa, and R. Mehran, "Calculation method for microstrip discontinuities and T-junctions," *Electron. Lett.*, vol. 8 pp. 177–179, Apr. 1972.

[2] G. Kompa, "*S*-matrix computation of microstrip discontinuities with a planar waveguide model," *Arch. Elek. Übertragung.*, vol. 30, pp. 58–64, Feb. 1975.

[3] W. Menzel and I. Wolff, "A method for calculating the frequency-dependent properties of microstrip discontinuities," *IEEE Trans. Microwave Theory Tech.*, vol. MTT-25, pp. 107–112, Feb. 1977.

[4] T. S. Chu, T. Itoh, and Y. C. Shih, "Comparative study of mode-matching formulations for microstrip discontinuity problems," submitted to *IEEE Trans. Microwave Theory Tech.* (Special issue on Numerical Techniques).

[5] R. Mittra and S. W. Lee, *Analytical Techniques in the Theory of Guided Waves*. New York: Macmillan, 1971.

[6] T. Itoh, "Spectral domain immittance approach for dispersion characteristics of generalized printed transmission lines," *IEEE Trans. Microwave Theory Tech.*, vol. MTT-28, pp. 773–736, July 1980.

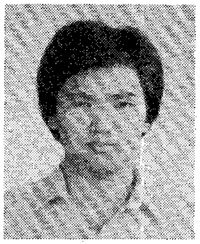

Tak Sum Chu was born in Kowloon, Hong Kong, on October 4, 1960. He received the B.S. degree in electrical engineering from the University of Texas at Austin in 1982. Currently, he is working towards the M.S. degree at the University of Texas.

Tatsuo Itoh (S'69–M'69–SM'74, F'82) received the Ph.D. degree in electrical engineering from the University of Illinois, Urbana, in 1969.

From September 1966 to April 1976, he was with the Electrical Engineering Department, University of Illinois. From April 1976 to August 1977, he was a Senior Research Engineer in the Radio Physics Laboratory, SRI International, Menlo Park, CA. From August 1977 to June 1978, he was an Associate Professor at the University of Kentucky, Lexington. In July 1978, he joined the faculty at the University of Texas at Austin, where is now a Professor of Electrical and Computer Engineering and Director of the Electrical Engineering Research Laboratory. During the summer 1979, he was a Guest Researcher at AEG-Telefunken, Ulm, West Germany. Since September 1983, he has held the Hayden Head Centennial Professorship of Engineering at the University of Texas. Since September 1984, he has been Associate Chairman for Research and Planning of Electrical and Computer Engineering Department.

Dr. Itoh is a member of the Institute of Electronics and Communication Engineers of Japan, Sigma Xi, and Commission B of USNC/URSI. He serves on the Administrative Committee of IEEE Microwave Theory and Techniques Society and is the Editor of IEEE TRANSACTIONS ON MICROWAVE THEORY AND TECHNIQUES. He is a Professional Engineer registered in the State of Texas.